The 2006 Eruption of Augustine Volcano, Alaska
Power, J.A., Coombs, M.L., and Freymueller, J.T., editors
U.S. Geological Survey Professional Paper 1769

Chapter 5

Earthquake Waveform Similarity and Evolution at Augustine Volcano from 1993 to 2006

By Heather R. DeShon[1], Clifford H. Thurber[2], and John A. Power[3]

Abstract

Temporal changes in waveform characteristics and earthquake locations associated with the 2006 Augustine eruption and preeruptive seismicity provide constraints on eruptive processes within the edifice. Volcano-tectonic earthquakes occur within the upper 1 to 2 km at Augustine between and during eruptive cycles, and we use the Alaska Volcano Observatory hypocenter and waveform catalog from 1993 to 2006 to constrain changes in event similarity and location over time. Waveform crosscorrelation with bispectrum verification improves the pick accuracy of the catalog data to yield better locations and allows for identification of families of similar earthquakes. Event waveform similarity is low at Augustine, with ~60 to 70 percent of events failing to form event families of more than 10 events. The remaining earthquakes form event families over multiple time scales. Events prior to the 2006 eruption exhibit a high degree of similarity over multiple years. Earthquakes recorded during the precursory and explosive phases of the 2006 eruption form swarms of similar earthquakes over periods of days or hours. Seismicity rate and event similarity decrease rapidly during the explosive and effusive eruption phases. The largest recorded swarms accompany reports of increased steaming and explosive eruptions at the summit. Relative relocation of some event families indicates upward migration of activity over time, consistent with magma transport by way of an ascending dike. Multiple regions of the edifice generate seismicity simultaneously, however, suggesting the edifice contains a network of fractures and/or dikes.

Introduction

Augustine Volcano is the youngest and historically most active volcano in the Cook Inlet region of Alaska. The edifice is composed primarily of andesitic material and forms a small island with a summit peak at 1.25 km above sea level. Past sector failures of the edifice have excited tsunamis in Cook Inlet. Major eruptions have taken place in 1883, 1935, 1963–64, 1976, 1986, and 2006, and these explosive eruptions created ash-rich plumes that posed significant hazard for overlying aircraft flight paths. The three most recent eruptions have followed similar eruptive sequences: (1) a precursory period of seismic unrest; (2) an explosive phase marked by one or more pyroclastic flow-generating eruptions; and (3) one or more dome-building effusive phases (Power, 1988; Power and Lalla, this volume). Most seismicity recorded at Augustine is volcano-tectonic (VT) in nature, with high-frequency P onsets indicative of shear failure in brittle material, and is confined to the upper 1 to 2 km of the edifice, with limited evidence for activity at 3 to 4 km below mean sea level (b.m.s.l.) (Kienle, 1987; Power, 1988; Power and Lalla, this volume). Low-frequency events associated with fluid processes are less common (Buurman and West, this volume). Magma transport during eruptive cycles at Augustine likely occurs through shallow dike propagation, with new eruptive cycles occurring as a result of an influx of juvenile magma at the base of the system (Cervelli and others, 2006; Roman and others, 2006).

Dike propagation at volcanoes frequently couples with increased rates of seismicity, and seismic monitoring provides useful early warning of major changes within volcanic systems (see McNutt, 2005, for a recent review). Because of the volcanic, seismic, and tsunami hazard posed by Augustine eruptions, the volcano has been seismically monitored since 1970. The Alaska Volcano Observatory (AVO) has maintained digital waveforms recorded by a network of five to eight short-period and broadband seismometers since 1993

[1]Center for Earthquake Research and Information, University of Memphis, 3890 Central Ave., Memphis, TN 38138.

[2]Dept. of Geoscience, University of Wisconsin-Madison, 1215 W. Dayton St., Madison, WI 53706.

[3]Alaska Volcano Observatory, U.S. Geological Survey, 4200 University Drive, Anchorage, AK 99508.

(fig. 1). Volcano seismic networks typically have few stations and marginal geographic coverage, and waveforms recorded at volcanoes are often noisy because of the complex interactions of tectonic and magmatic processes, wind, and poor site conditions. As a result, onset pick accuracy may be highly variable within a phase catalog. Routine catalog locations at Augustine exhibit a high degree of scatter within the shallow edifice that complicates interpretation of magmatic and hydrothermal processes. Scatter may be an artifact of location procedure or imprecise phase onset picks, or it may be a real feature of volcanic activity. Catalog earthquake locations at Augustine are calculated using analyst phase picks and an approximate, one-dimensional (1*D*) velocity model with station corrections developed for Augustine (Power, 1988). More than 3,800 events have been catalogued at Augustine from 1993 through 2006 (Dixon and others, 2008), and ~2,000 of these were related to the 2006 eruptive sequence (fig. 1).

Retrospective analyses of volcano seismic data using waveform crosscorrelation methods can provide insight into the relative similarity of waveforms in time and space, which in turn can reflect the underlying eruptive processes (for example, Got and others, 1994; Rubin and others, 1998; Battaglia and others, 2004; Rowe and others, 2004; DeShon and others, 2007). In this study, waveform crosscorrelation techniques are applied to the seismic event archive for Augustine Volcano extending from 1993 through December 2006. Identification of characteristic families of similar earthquakes provides a clearer picture of how seismicity evolves within the edifice before and during eruptive cycles at Augustine Volcano. We examine temporal changes in waveform characteristics associated with the 2006 Augustine eruption and preeruptive seismicity and identify families of similar earthquakes that occur at multiyear, multimonth, multiday, and multihour timescales. Relative location of selected event families associated with the precursory and explosive phases of the 2006 eruption provides insight into seismic and magmatic processes occurring at Augustine Volcano.

Method

Waveform Crosscorrelation

If two events are closely located in space and share similar source mechanisms, they should generate similar ground motions and be recorded as similar waveforms. Waveform crosscorrelation (CC) of two events recorded at the same station yields: (1) a maximum absolute value of the CC coefficient that varies between 0 and 1, where 1 represents a perfect waveform similarity; and (2) an associated relative time delay or lag

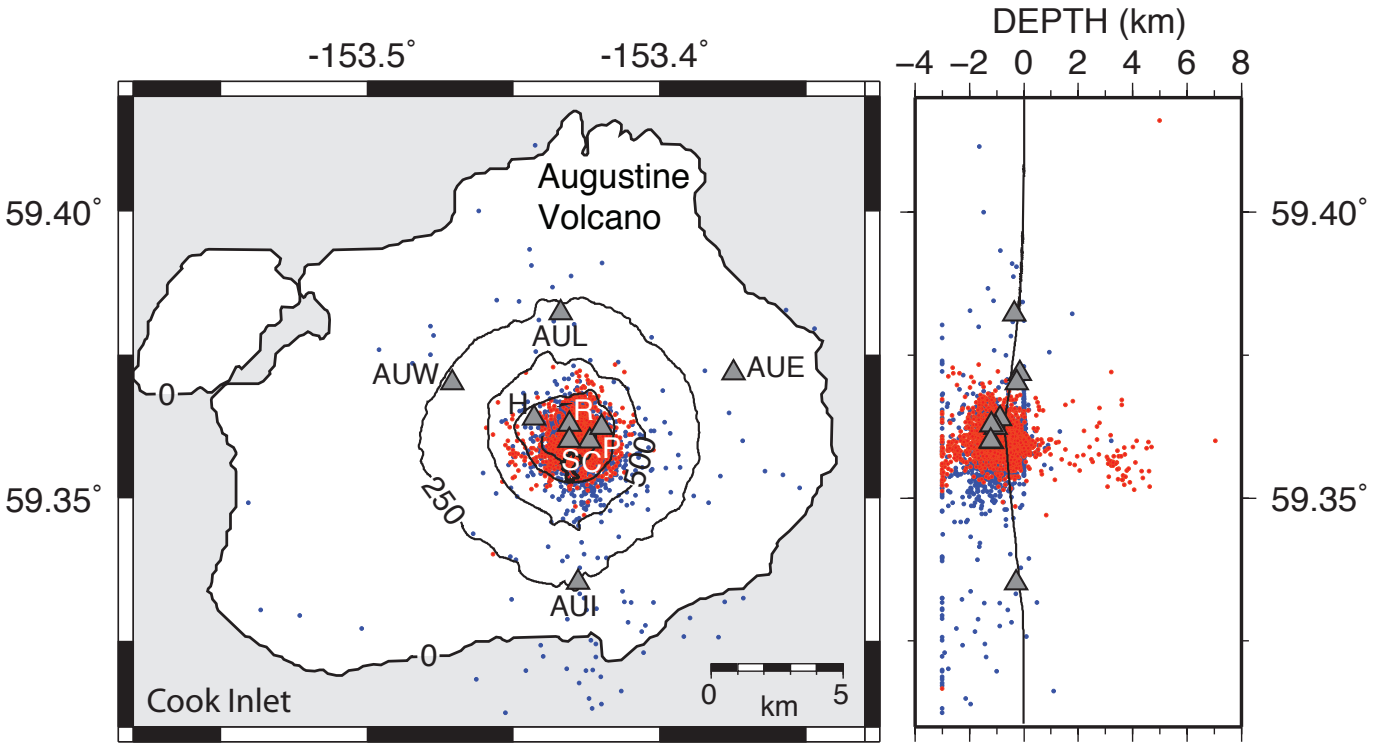

Figure 1. Map view and north-south oriented cross-section of Augustine Volcano. Contour interval is 250 m. Triangles are AVO seismic stations used for waveform crosscorrelation. The "AU" has been left off of the summit stations for drafting clarity. Blue dots are AVO catalog events occurring from 1993 to April 2005. Red dots are AVO catalog events occurring on and after April 2005.

reflecting the time shift necessary to best align the waveforms. High-quality time delay estimates can be identified by finding a threshold value for the CC coefficient that maximizes the number of correlated arrivals while minimizing the number of false-positive correlations (for example, Schaff and others, 2002). Correlation lag estimates can be used to correct inconsistent picks and revise absolute arrival times (for example, Dodge and others, 1995; Dodge, 1996; Shearer, 1998; Aster and Rowe, 2000; Rowe and others, 2002a). CC coefficients contain valuable information on event similarity and can be used to identify families of similar waveforms (Rowe and others, 2002a).

CC coefficients may be low if the underlying signals are not time-delayed similar waveforms, or if high levels of noise contaminate the underlying time-delayed signals. In the presence of correlated Gaussian noise, traditional CC methods may provide low coefficients for similar events, or high correlations with the estimated correlation lag driven by the correlated noise, rather than the signal of interest (Du and others, 2004). Correlated or partially correlated noise may result at individual stations because of a combination of constant predominant noise sources such as wind and site response effects. Bispectrum crosscorrelation (BCC), or CC in the third-order spectral domain, suppresses correlated Gaussian noise or low-skewness noise sources (Nikias and Raghuveer, 1987; Nikias and Pan, 1988; Yung and Ikelle, 1997) and can effectively identify the global CC time shift in cases where traditional methods fail because of correlated noise contamination. BCC produces time delay estimates consistent with traditional second-order spectral domain methods when noise is not correlated (Du and others, 2004).

The bispectrum crosscorrelation package for seismology (BCSEIS) verifies traditional CC time delay estimates by additionally computing a BCC lag prediction for filtered and unfiltered waveforms (Du and others, 2004). The use of BCSEIS with Augustine data closely follows the approach outlined for data from Redoubt Volcano, Alaska (DeShon and others, 2007). For Augustine data, the BCSEIS verification threshold was set to twice the sampling interval, and waveforms were filtered using a three pole, two pass, Butterworth bandpass filter with a low frequency corner at 1 Hz and a high frequency corner at 20 Hz. CC was performed using a window extending from 0.3 seconds before to 0.7 seconds following the P-wave arrival (fig. 2). This window was large enough to allow CC of the P-wave coda to identify similar families of earthquakes and incorporate large mispicks. The bulk of seismicity is small magnitude, near-summit events with high frequency P onsets and no discernable S-wave arrivals as recorded on the vertical component, short period summit stations. At the summit stations, the CC window may contain P and S wave information. We were primarily interested in identifying families of similar earthquakes, however, and crosscorrelation of P or P and S energy does not significantly bias our results.

Event Clustering and Pick Adjustments

We identified families of similar earthquakes using the verified CC coefficients and a dendrogram-based, hierarchical pair-group algorithm (Rowe, 2000; Rowe and others, 2002a). CC coefficients are used to fuse event pairs with high

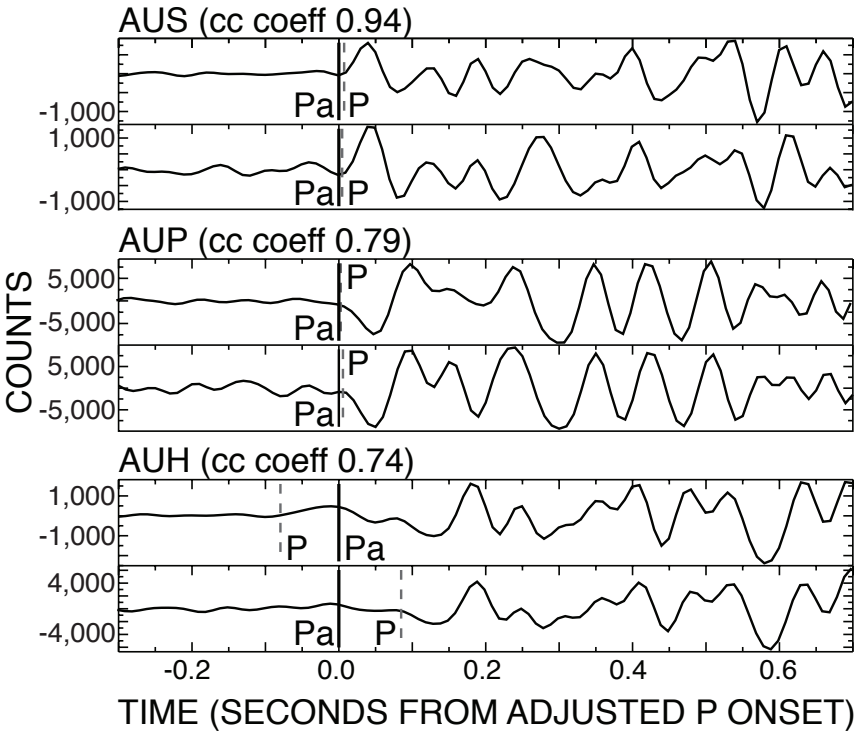

Figure 2. An example of bispectrum crosscorrelation package for seismology (BCSEIS) analysis for two Augustine earthquakes. The waveforms are aligned on the adjusted P onset (Pa) based on crosscorrelation (CC) and event clustering results. The original catalog P onset (P) is also marked. The associated CC coefficient for each event pair is shown next to the station name. Event pairs at each station with CC values ≥0.79 are automatically accepted for use with clustering techniques. Event pairs with CC values ≥0.30 are accepted if at least one other station reports a CC value ≥0.88 for the same data. For this event pair, CC coefficients and predicted lag estimates at AUS, AUP, and AUH would be accepted.

waveform similarity into clusters, and clustering is considered complete when a user-defined CC coefficient cutoff threshold is reached (see Rowe and others, 2002a, for further details). For the Augustine data, this threshold was set to 0.80. The set of time delays associated with each intracluster event pair, weighted by the associated standard deviation calculated during waveform CC, are inverted to solve for a set of phase onset corrections. Inversion is calculated using an iterative, conjugate gradient approach that minimizes the L1-norm misfit (Aster and Rowe, 2000; Rowe and others, 2002a).

We used the above process to solve for clusters or multiplets of highly similar waveforms at all stations within the Augustine network. Event pairs with BCC-verified CC values ≥0.79 were used during event clustering. Additionally, for a given event pair, if at least one station has a verified CC coefficient ≥0.88, then other stations need only have a verified CC coefficient ≥0.30 to also be included in the clustering analysis. Augustine events primarily separate into small clusters with fewer than six events, and approximately one-third of events do not get included in any cluster. This suggests that discrete, dissimilar earthquakes and/or noisy waveforms dominate the Augustine catalog. Visual analysis of clusters containing six or more events suggested that some could be combined to form larger clusters with similar, but not identical, waveforms. We combined like clusters and grew clusters by incorporating events that may have one or more verified and reported lag adjustments to other cluster members; these new events were confirmed as new cluster members by visual comparison. Clusters were then compared across the network to identify event families, or sets of events that generated similar waveforms at all stations (fig. 3). We interpret those families with ≥10 member events in this report.

Results

The seismic record at Augustine Volcano recorded from 1993 to 2005 is dominated by small-magnitude shallow edifice events occurring at rates as high as 54 events/month (fig. 4). Approximately 60 to 70 percent of recorded events are not associated with event families containing more than 10 earthquakes, based on waveform similarity measured by crosscorrelation. Waveform dissimilarity is the dominant feature of catalog seismicity. Waveform similarity, when present, increases with small accelerations in seismicity rate (fig. 4). The resulting families of similar earthquakes contain multiplets of temporally related events over short time scales (days and hours). The similarity of some of the sets of multiplets over longer periods of time (years and months) suggests that intrafamily clusters share source location and process and that some regions of the edifice may be reactivated.

Before the seismicity rate increase in April 2005, event families contain 10 to 20 events (fig. 4*A*), with similar waveforms separated in time by months to years. Figure 5 illustrates a typical event family extending from late 1998 to late 2000 (family S in fig. 4*A*). The family consists of 4 events in 1998, 5 events in 1999, and 10 events in 2000. Waveforms exhibit similarity in P onset, suggesting a similar location, source, and/or path, especially at summit stations AUP and AUH. Waveform similarity in the P coda at summit station AUR is not as high as at the other recording summit stations, which may be indicative of changes in path characteristics over time. As the seismicity rate increases during the early precursory stage in April 2005, event families occur over months and weeks rather than years (fig. 4*B*).

Family LM is an interesting example of both a long-term (year) and mid-term (month) time scale for waveform similarity. The family extends from 1997 through 1998 and reappears from 2004 through 2005 (figs. 4*A*, 4*B,* 6). The set of waveforms was originally identified as two separate clusters because of the opposite sign of the P onset at AUS (fig. 6); however, the seismometer at station AUS was replaced on September 19, 2003, at which point the orientation of the vertical channel was reversed. Waveforms in this family have a highly similar P onset on the summit stations but more variable P coda characteristics. Coda similarity is highest within the temporally related swarms that make up the family (fig. 6). The overall similarity of the waveforms suggests that the same region of the edifice was active throughout much of 1998 during a brief increase in seismicity rate and again during the precursory stages of the 2006 eruption (fig. 4*A*).

During November and December 2005, seismicity rate increases significantly, and the time scale of event similarity switches from years and months to weeks and days (fig. 4*C*). The average size of the families does not change significantly and consists of 10–20 events. Swarms of similar earthquakes occur over periods of hours and days followed by periods of quiescence. The same area of the edifice may reactivate days to weeks later, as illustrated by the time separation between events in families AI and AC (figs. 4*C*, 7). We also identified small swarms of highly similar events that appear to grade into one another over a period of days. This behavior is illustrated in figure 8 using families C, BC, and B, which occur during a period of increased seismicity from December 9 to 11, 2005 (fig. 4*C*). Individually, each family of ~15 events contains highly similar waveforms that occur over a period of hours. The P onset at each of the summit stations suggests a highly similar source process or location, but the P coda remains distinct between families (fig. 8). Over this same time period, events occur in other regions of the edifice, generating P onsets with opposite sign (fig. 9).

The shortest duration family consists of a swarm of ~70 similar earthquakes on January 11, 2006, from ~2000 to 2200 AKST (Alaska Standard Time) (family AD, fig. 4*C*). These events were recorded between the first two stages of explosive activity on January 11 and 13, 2006. Though these events are highly similar, the waveforms evolve over time, likely reflecting small changes in source process, source location, changes in path characteristics, or some combination of factors (fig. 10). Following this swarm, ~30 events with a similar high-frequency content but different onset and coda characteristics were recorded at the summit stations (family AH, figs. 4*C*,

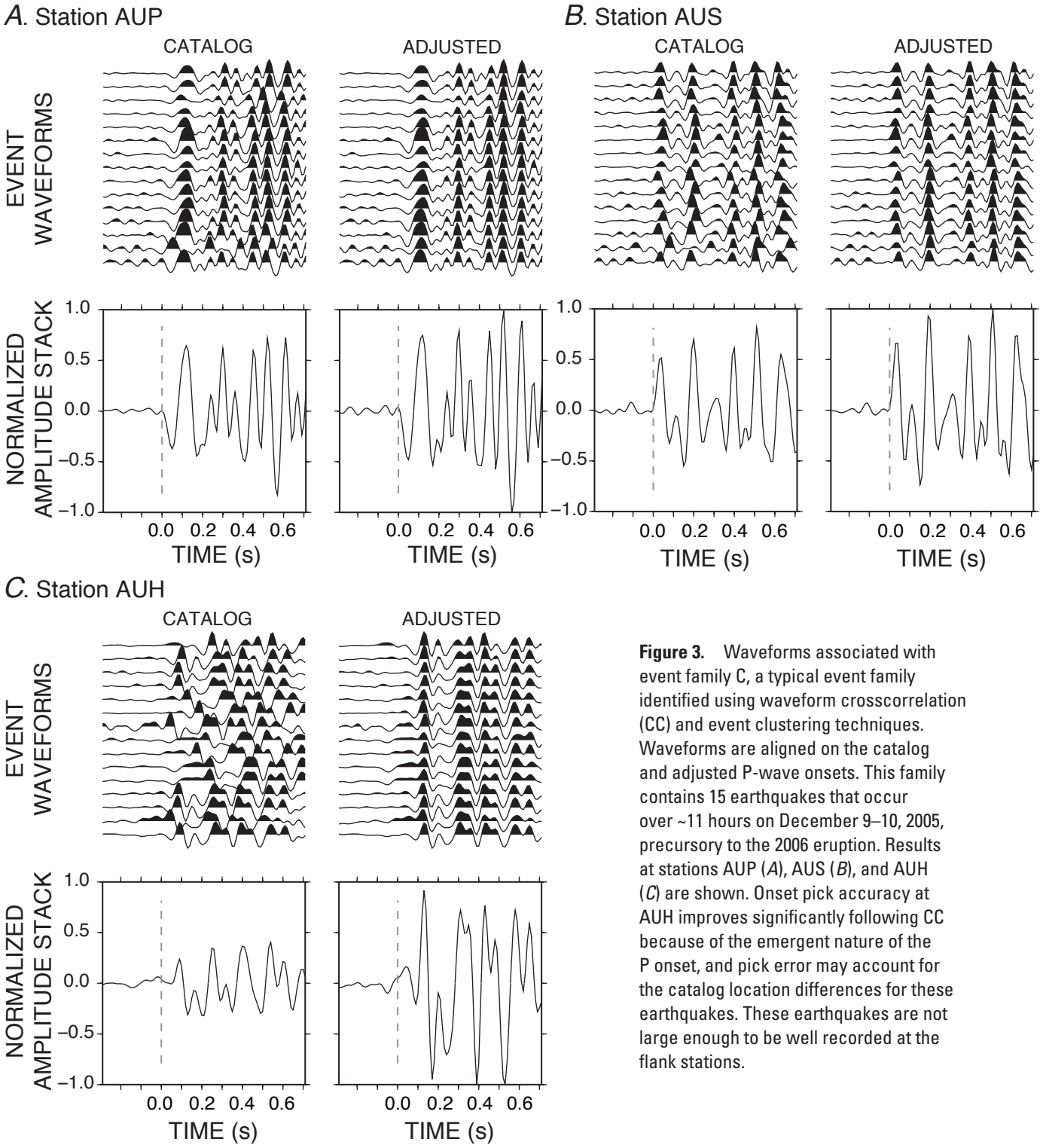

Figure 3. Waveforms associated with event family C, a typical event family identified using waveform crosscorrelation (CC) and event clustering techniques. Waveforms are aligned on the catalog and adjusted P-wave onsets. This family contains 15 earthquakes that occur over ~11 hours on December 9–10, 2005, precursory to the 2006 eruption. Results at stations AUP (*A*), AUS (*B*), and AUH (*C*) are shown. Onset pick accuracy at AUH improves significantly following CC because of the emergent nature of the P onset, and pick error may account for the catalog location differences for these earthquakes. These earthquakes are not large enough to be well recorded at the flank stations.

11). These events were not well recorded on the flank stations, however, so the catalog location quality is poor.

Events within each family exhibit waveform similarity that should correspond to spatial similarity, but catalog locations for events within individual families generally have a high degree of scatter. For example, family AD waveforms are linked by an average CC coefficient of 0.92 at station AUP, but the catalog depths for these events range from –3.0 to 0.0 km b.m.s.l. Events with identical source process and location should also exhibit identical differences in absolute arrival time between any two stations. This differential arrival time is independent of origin time but is sensitive to changes in path velocity over the time between earthquakes. For swarm activity over small time scales, we can assume the velocity

along the path from earthquake to station does not change significantly, and we can use differential arrival times to prove colocation. We present an example of this process using family AD. We calculated the difference in absolute arrival time between summit station AUP and (1) summit station AUH; (2) flank station AUL; and (3) flank station AUW (fig. 12). These four stations exhibit high signal-to-noise ratio for events in family AD (fig. 10). We removed the median value of the differential times to find a time residual; residuals should be zero for colocated earthquakes. For family AD, the time residuals for each station-pair have a zero mean and scatter is small (fig. 12). The increased scatter in time residuals for AUP-AUL reflects the relatively poorer recording of these earthquakes at station AUL (fig. 10).

The mean differential arrival times for sets of station-pairs for each family contain information on relative locations between families. If families are separated in space, then the differential time median at any given station-pair should differ. In figure 13, we show the relationship between median differential times for station-pairs AUP-AUH, AUP-AUW, and AUP-AUL. Because of the assumption that path velocity does not vary over time, we show only event families with relatively short durations that occur during the 2006 Augustine eruption. Family AD, which occurred during the explosive phase, clearly separates from families A, B, BC, and C that occurred during the early precursory phase in November and December 2005 (fig. 13). The spatial similarity between the December 2005 events is consistent with the high degree

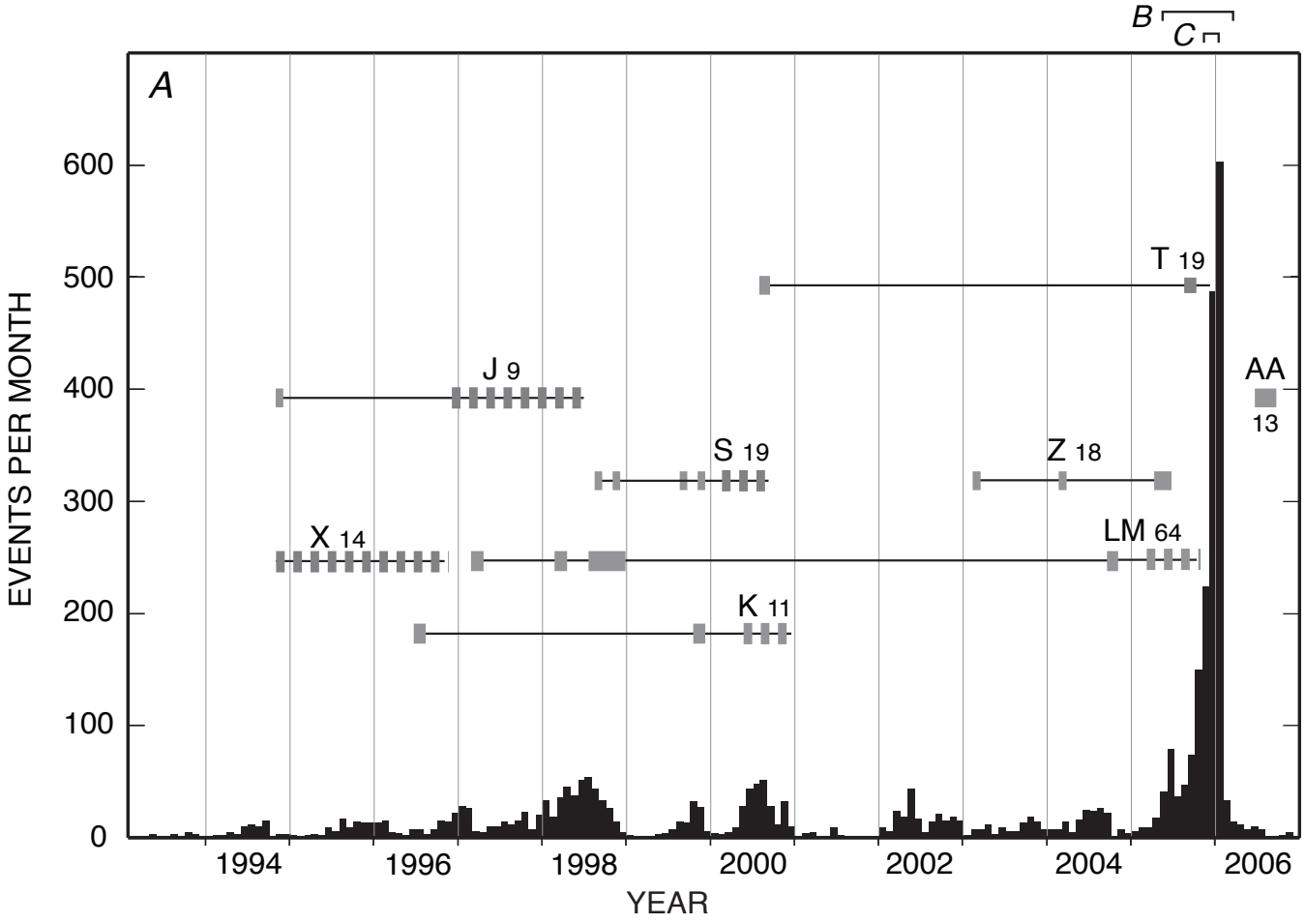

Figure 4. Seismicity rate and event families identified using the Augustine Alaska Volcano Observatory (AVO) catalog. On each panel, the histogram indicates seismicity rate over time and horizontal black lines indicate the extent in time of waveform families. Family names are indicated by letters and are followed by the number of member events. Solid squares represent time periods over which multiplets of earthquakes occur within each family. *A*, Histogram of the number of catalog earthquakes per month from 1993 to 2006. Event families with a time range on the month to year scale are shown. Bars indicate the time periods shown in panels *B* and *C*. *B*, Histogram of the number of catalog earthquakes per day during the 2006 eruption and precursory period. Seismicity rate decreases significantly following explosive eruptions in January 2006. Bar indicates the time period shown in panel *C*. *C*, Histogram of number of catalog earthquakes per day in November and December 2005, and in January 2006. Arrows mark periods of explosive, plume-forming eruptions. Black: first motion down at AUP. Gray: first motion up at AUP.

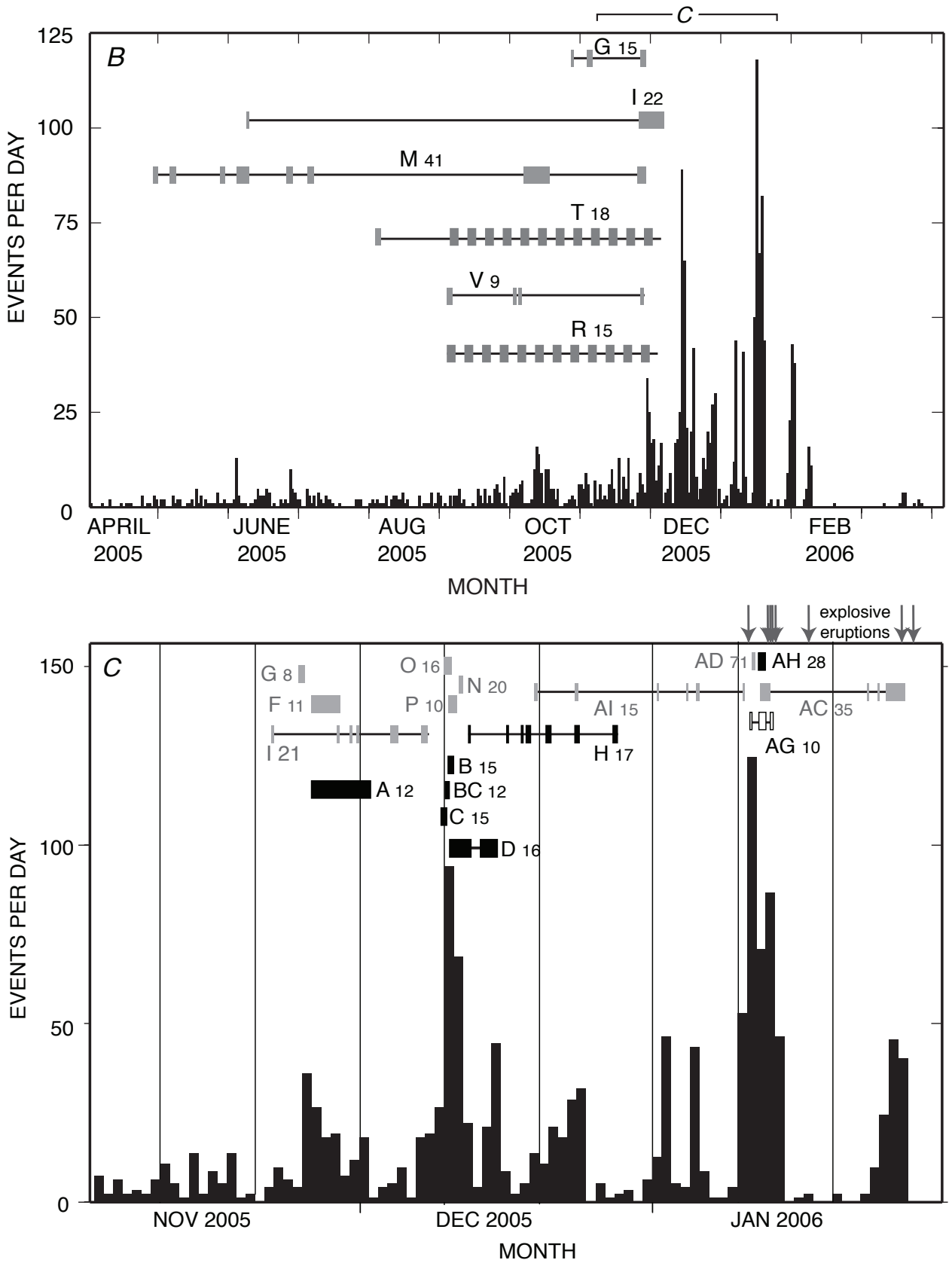

Figure 4.—Continued.

of intracluster waveform similarity between these clusters (fig. 8). On the basis of network geometry, the lower values for AUP-AUW and AUP-AUL for family AD likely indicate a shallower depth for these events relative to the other families. Shallow events should generate higher differential arrival times between summit and flank stations than events within the edifice near sea level because the sea level, events are actually closer to the flank stations than to the summit stations. Clusters O and N occur over the same period of time as families B, BC, and C but have opposite first motion polarity at AUP (fig. 9), and they appear separated in this diagram. This relationship suggests that multiple regions of the edifice can be simultaneously active.

We can further take advantage of the differential arrival-time medians for each cluster by inverting these data to solve for relative locations between families when families are well recorded on more than three stations. This location methodology is a variant of the method of hyperbolas (Milne, 1886) and the related equal-differential-time method (Zhou, 1994). To test this method, we relocated families A, B, and AD and used all station-pair combinations of summit stations AUP, AUS, and AUH and flank stations AUL and AUW. We solved for an initial cluster location by computing the misfit between the set of observed and calculated station-pair differential times. We solved for the location that minimizes the station-pair residuals, applying weighting to stabilize the inversion.

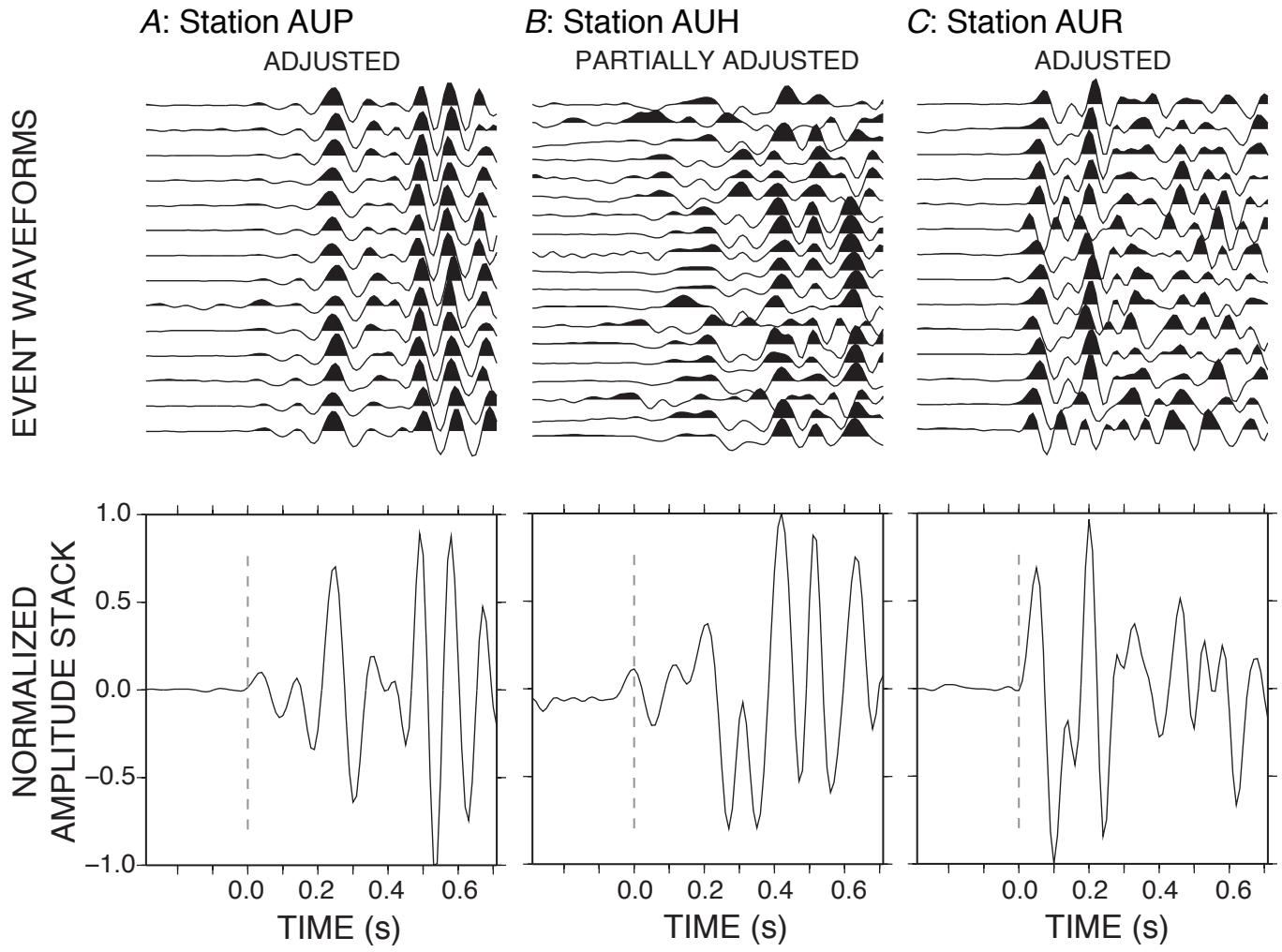

Figure 5. Waveforms and normalized amplitude stacks for event family S, which occur from June 22, 1998, through September 23, 2000 (see fig. 4*A* for full time extent), at stations AUP (*A*), AUH (*B*), and AUR (C). Waveforms are shown aligned on adjusted P onset and filtered between 1 and 20 HZ (upper panel) and as an normalized amplitude stack (lower panel). At all summit stations, such as the examples at AUP and AUR, the waveforms exhibit similarity in P onset, suggesting a similar location, source and path, but they are not identical. Because of the emergent nature of P onset at AUH, pick quality in the initial catalog was poor. The number of verified time delays between all possible event pairs was not sufficient for the inversion process to correctly adjust P onsets at this station.

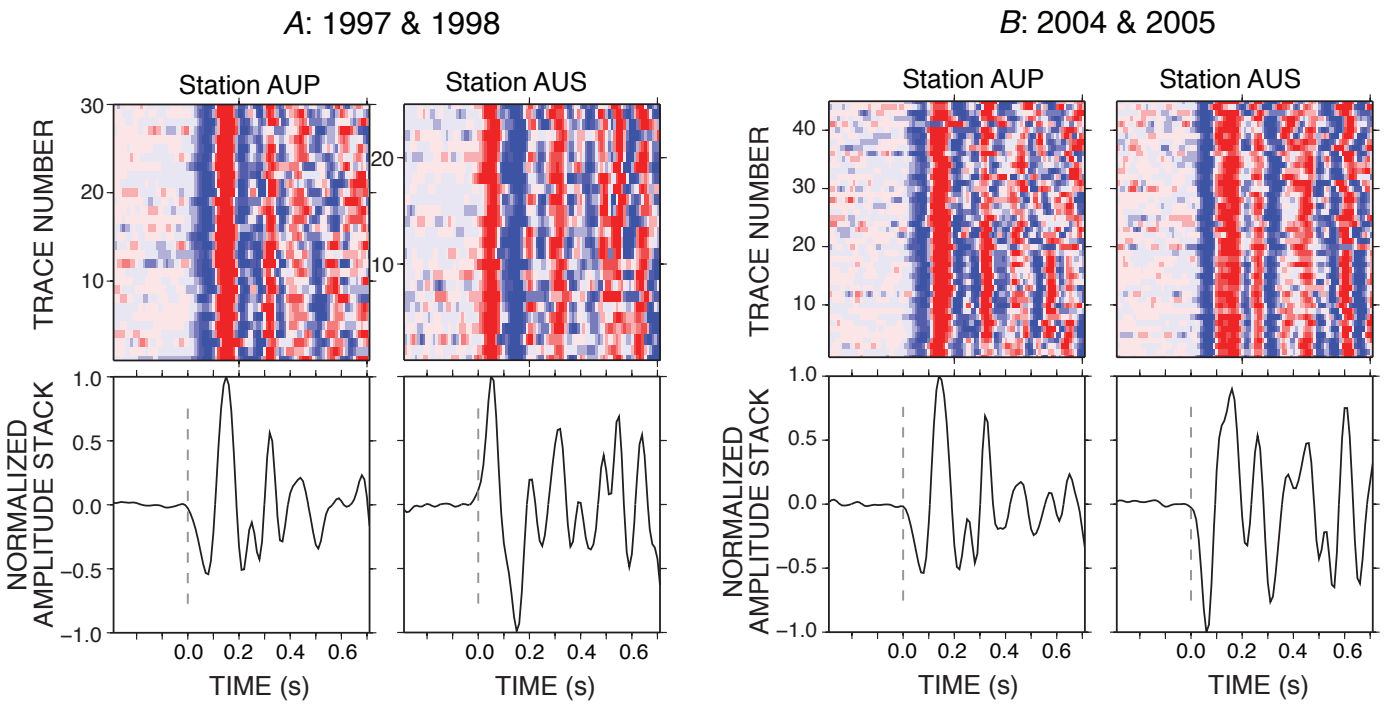

Figure 6. Waveforms for family LM recorded at summit stations AUP and AUS. A, Events from 1997 through 1998. B, Events from 2004 through 2005. Though the waveforms at AUS have different first motion P onsets, this reflects a change in vertical component orientation and not a change of source. Upper panels: Waveforms are visualized as wigglegrams (Rowe and others, 2002b), where red indicates positive and blue indicates negative normalized amplitude. Color intensity scales with normalized amplitude. Waveforms are aligned on the adjusted P onset and sorted by time (trace 1 being the earliest occurring event). Lower panels: Stack of amplitude normalized waveforms. The dashed line indicates P onset. Wigglegrams are used throughout this study to visualize families with more than 20 member events.

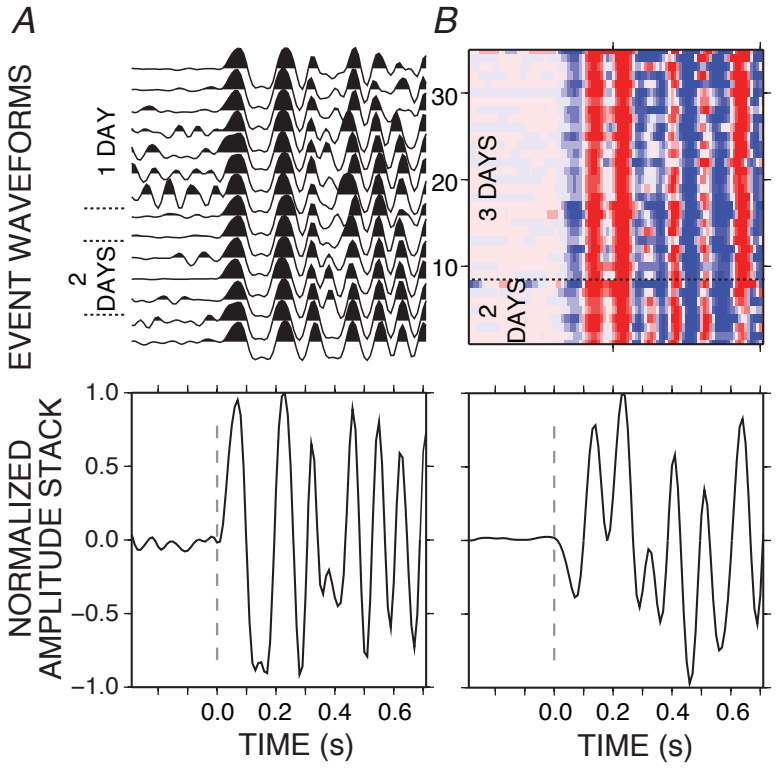

Figure 7. Waveforms and stacks for family AI at summit station AUP (*A*) and family AC at summit station AUH (*B*). Events making up these two families recur over multiple weeks (see fig. 4*B* for full time extent). Each family consists of subsets of single or multiplets of earthquakes that occur over much shorter time scales (one to three days), as noted by small dashed lines on the upper panel. Upper panels: Waveforms are aligned on the adjusted P onset and sorted by time. Family AC contains more than 30 events and is shown as a wigglegram. Lower panels: Stack of amplitude normalized waveforms. The dashed line indicates P onset.

Summit-to-summit times were assigned weight 1.0, and summit-to-flank and flank-to-flank stations were set to 0.02. We assumed a constant velocity half space of 3.5 km/s for P waves, which is slightly faster than the average edifice velocities in the 1D AVO velocity model for Augustine. Edifice velocities are poorly constrained at Augustine, however, and there is some evidence that edifice velocities may be as high as 4.4 km/s (Power, 1988). Families A and B are separated by ~100 m, but more significantly are located 400 m to the south, 200 m to the east, and 800 m deeper than family AD, which is associated with explosive eruptions.

Sumiejski and others (2009) extended this approach of using station-pair differential times to derive family locations for the 2006 Augustine eruption. They used the CC coefficients derived in this study for nine families (A, AC, AD, AH, B, BC, C, LM, and O) using all 36 Augustine station-pairs and incorporated a linear-gradient velocity model obtained from preliminary forward modeling of the data. They also calculated quality weights for each of the station-pair time differences and solved for location using both a grid search and a modified Geiger's method of iterative, reweighed least squares (see Sumiejski and others, 2009, for further information). The results indicated that family LM occurs at ~300 m b.m.s.l. Precursory activity A, B, BC, and C located at ~500 m above m.s.l. (a.m.s.l.), as does family AC that is associated in time with the explosive phase. Families AD and AH, also associated with the explosive phase, located near the Augustine summit at ~1,200 m a.m.s.l.

Deep events (below ~3 km b.m.s.l.) are fairly rare at Augustine. Fifty-four catalog events occur between 2.5 and 6 km b.m.s.l. at Augustine, and all but five of these occur in 2006. Power and Lalla (this volume) showed that all but 18 of these events are mislocated shallow earthquakes. Deep events at Augustine are not expected to be well recorded at summit stations (Lalla and Kienle, 1980), and most summit stations

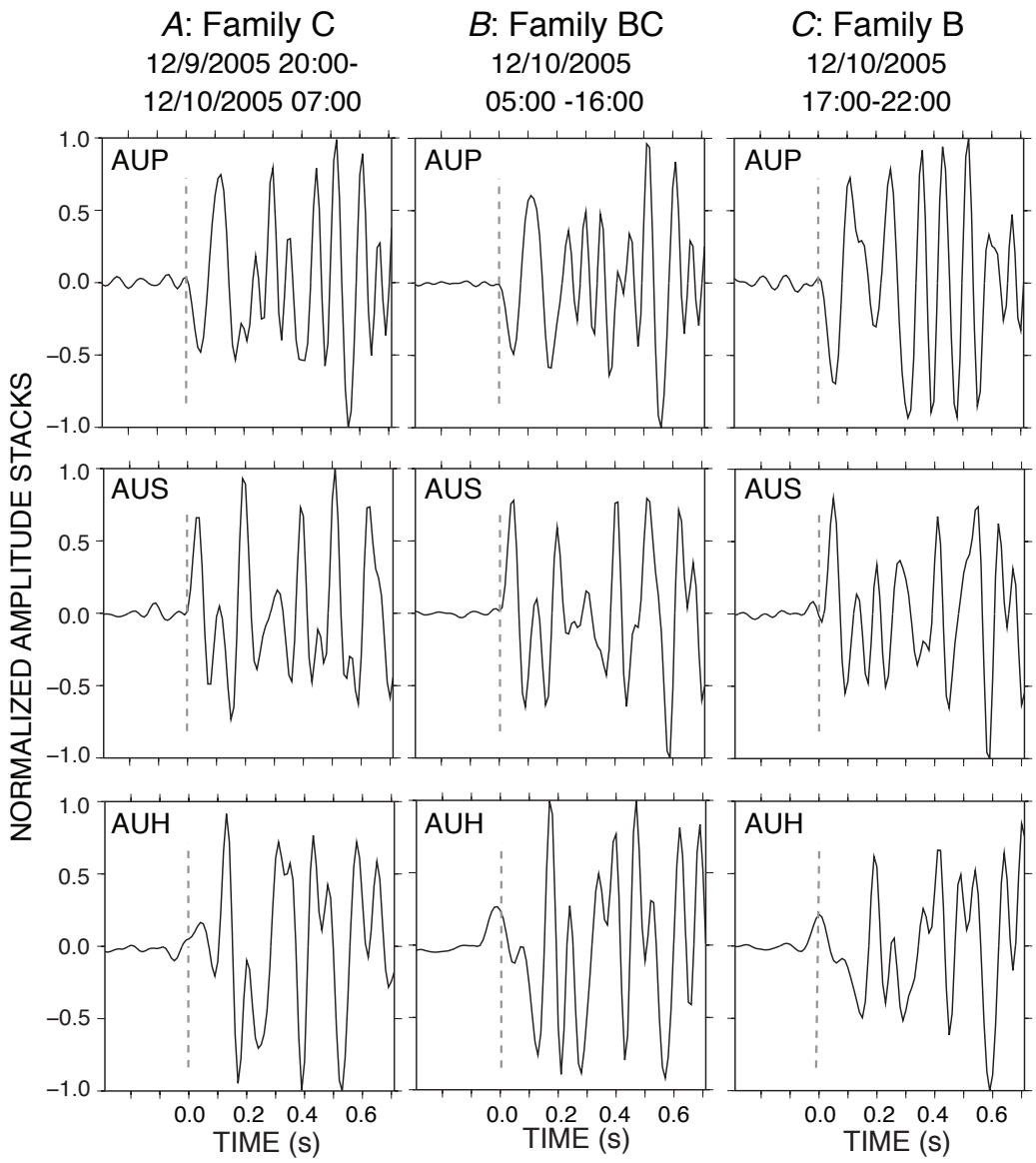

Figure 8. Normalized amplitude waveform stacks at stations AUP, AUS, and AUH aligned on adjusted P onset for event families C (*A*), BC (*B*), and B (*C*). These families occur consecutively in time during December 9–10, 2005, and the exact time extent of each is shown as date and hours AST. The event families are very similar in P onset and frequency content. Difference in P coda may be due to spatial migration or small changes in source mechanism. The mean centroid for each family is at ~ –0.68 km b.m.s.l.; the individual catalog hypocenter depth ranges are from –3 to 0 km b.m.s.l. The dashed line indicates P onset.

went offline following the explosive eruptions in January 2006. Of the remaining deep events, eleven of these events have fairly similar P onsets (fig. 14) and form event family AA (fig. 4*A*). The events occur throughout a 3-month period following the cessation of explosive activity. No deep seismicity was recorded during or following the 1986 Augustine eruption, although some activity was located at these depths before the 1976 eruption (Power and Lalla, this volume). Changes in network geometry between the 1976 and 1986 eruptions could account for this feature of the seismicity. Kienle (1987) interpreted seismicity occurrence at 3 to 4 km b.m.s.l. to be indicative of magma transport within or out of a storage body associated with the 1976 eruption. If a storage system is present at these depths and provided source material for the 2006 eruption, deep seismicity appears primarily linked to posteruptive processes.

Discussion

Seismic unrest prior to the 2006 eruption began as a steady increase in microearthquakes beneath the volcano, ranging from 1 to 2 events located in the AVO catalog per day in May of 2005 to 15 per day in mid-December. Over this period, continuous GPS (cGPS) sites located on the volcano flanks began to move away from one another in a radial manner, indicating inflation of the edifice. On November 17, 2005, the east-west baseline abruptly offset and motion at each station accelerated (Cervelli and others, 2006). On January 11, 2006, the eruption entered the explosive phase and generated the first of 13 explosive eruptions that continued throughout the month. During January 12–13, 2006, explosive eruptions ceased but seismicity rate reached a peak of 130 events/day (fig. 4*C*). At this time, a cGPS site located on the summit moved ~10 cm northeast. Six explosive eruptions commencing on January 13 and ending January 14, 2006, destroyed all summit seismic and cGPS stations. A large pyroclastic flow related to the January 28, 2006, explosive eruption buried the northernmost cGPS station and seismic stations AUL and AUH (fig. 1). Over February and March 2006, quieter magma effusion led to numerous pyroclastic flows, formation of a new lava dome, and magma flows on the north and northeast flanks. Seismicity rate returned to pre-2005 levels by late February 2006.

Cervelli and others (2006) modeled the Augustine cGPS data using an ascending dike source. They showed that the precursory-stage radial pattern recorded by the cGPS is consistent with an initial source with a top no higher than sea level. Mattia and others (2008) modeled the initial source as a vertical ellipsoid at ~300 m b.m.s.l. Summit cGPS data were well fit by a dike beginning to ascend on November 17 and reaching near the surface by mid-December 2005, likely coincident with increased edifice activity on December 9–11, 2005 (fig. 4*C*). The ascending dike likely did not breach the summit until the explosive eruption of January 13, 2006. The initial explosive eruption of January 11 contained no juvenile material, whereas the January 13 magmas were dominated by juvenile material (Wallace and others, this volume; Cervelli and others, 2006). This observation is consistent with the continuing motion recorded by the summit cGPS station through January 13, 2006.

The above model of the 2006 eruption is broadly consistent with a model for the 1986 eruption based on melt inclusion data (Roman and others, 2006). Roman and others (2006) found that the 1986 erupted magmas contained

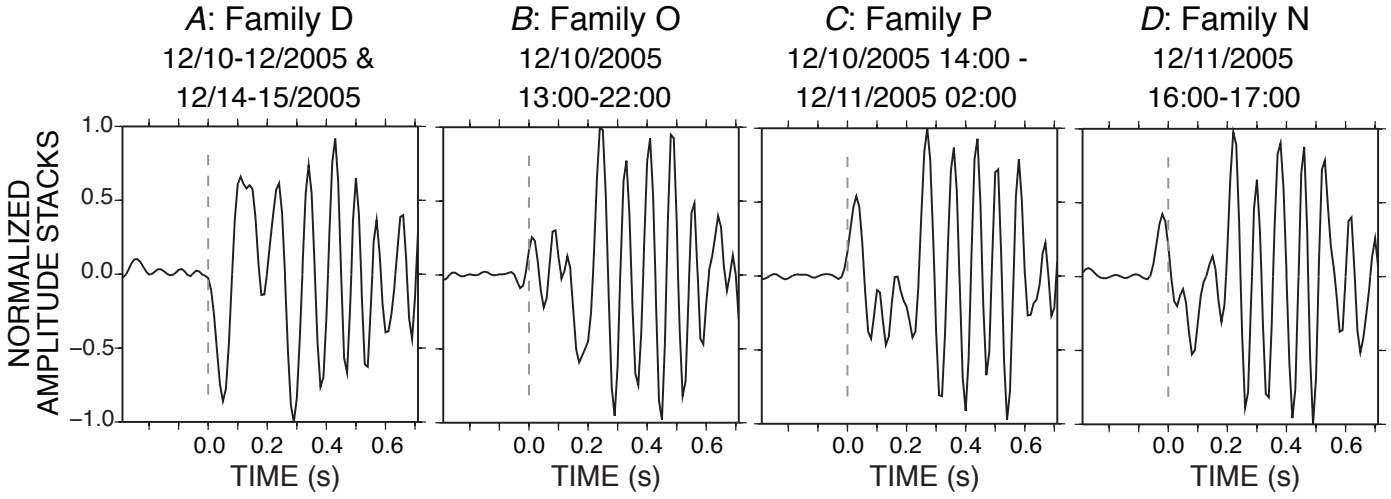

Figure 9. Normalized amplitude waveform stacks at station AUP for event families D (*A*), O (*B*), P (*C*), and N (*D*). These families occur from December 10 to 15, 2005, and hence overlap in time those shown in figure 8. Families O, P, and N have opposite first motion at AUP than either family D or families C, BC, and B (fig. 8). Similarly, the mean centroid of family D is –0.67 km b.m.s.l., much like that for the families shown in figure 8. Families O, P, and N have mean centroids of –0.62 km, –0.63 km, and –0.92 km b.m.s.l., respectively. This suggests that multiple regions of the edifice are generating volcano-tectonic earthquakes over the same temporal period. The time extent of each family is shown as date and hours AKST. The dashed line indicates P onset.

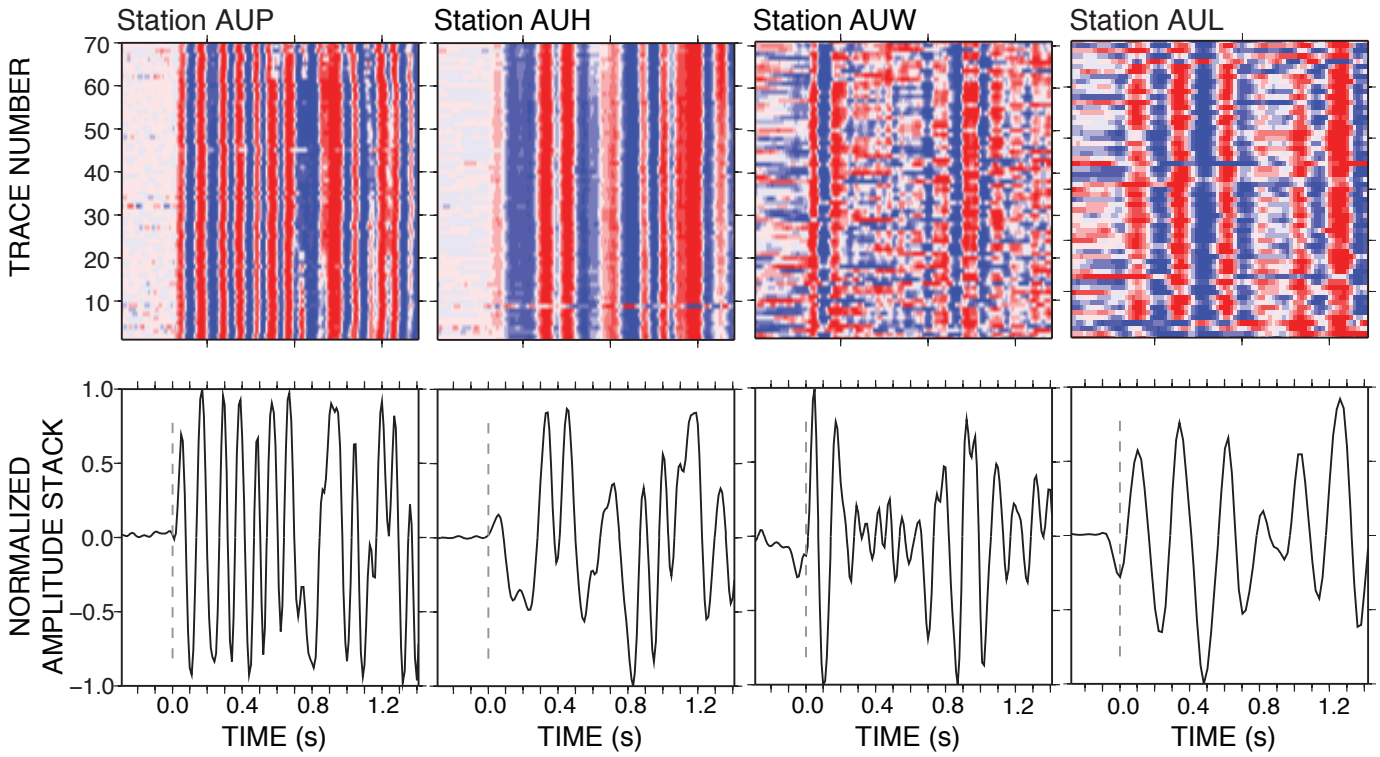

Figure 10. Wigglegrams and normalized amplitude waveform stacks for a swarm of ~70 earthquakes on January 11, 2006, which extended from ~2000 to 2200 AKST (family AD on fig. 4*C*). Waveforms are aligned on the adjusted P onset at summit stations AUP and AUH and at flank stations AUW and AUL. Though these events are highly similar, the waveform does evolve over time, likely reflecting small changes in source process or path. The dashed line indicates P onset.

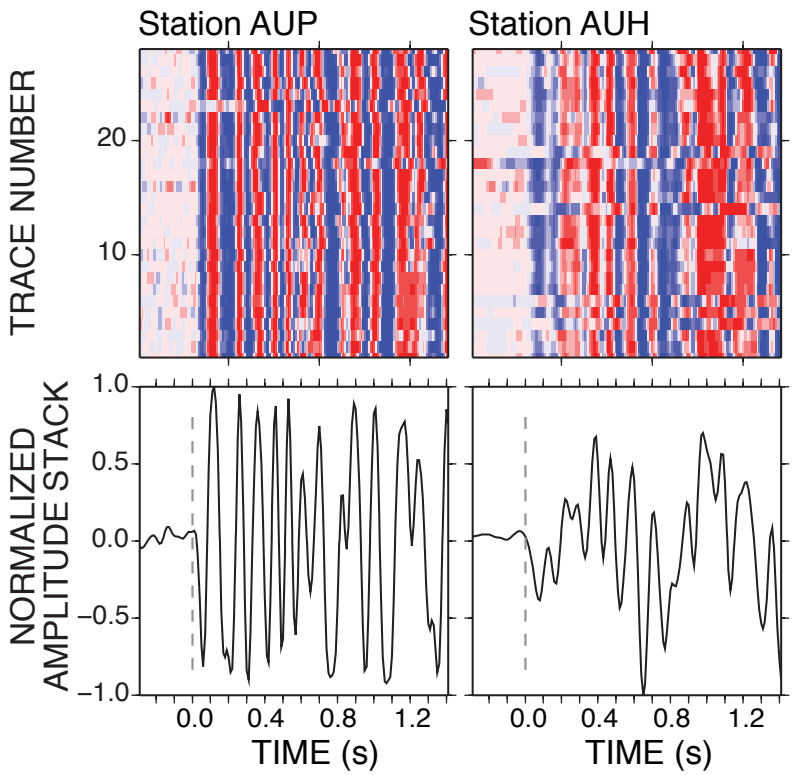

Figure 11. Wigglegrams and normalized amplitude waveform stacks for 28 similar earthquakes that occurred over a 13-hour period during the initial explosive stage (family AH on fig. 4*C*). Waveforms are aligned on the adjusted P onset at summit stations AUP and AUH. These events start to occur a few hours after the large swarm shown in figure 10 and contain the same overall frequency content of the larger swarm. However, first motion polarity is opposite. The dashed line indicates P onset.

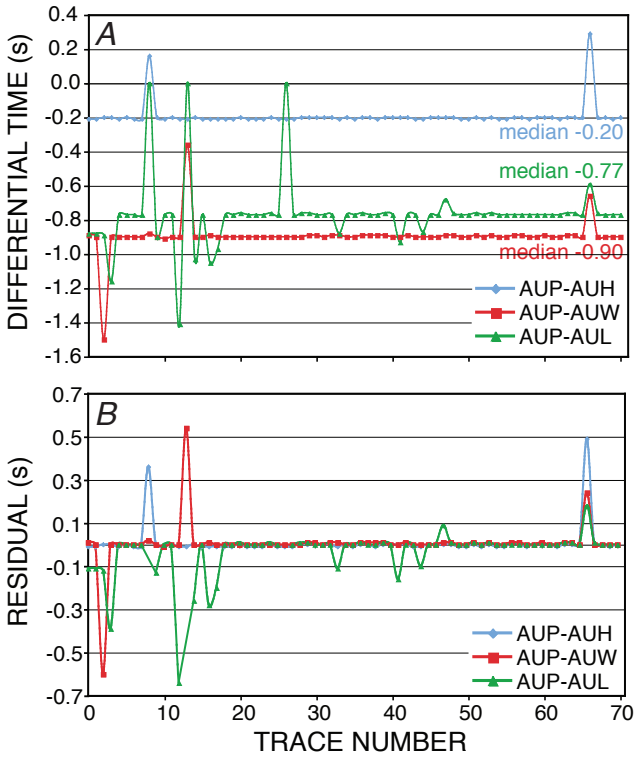

Figure 12. Collocated events should generate identical arrival-time differences at any two stations, as shown here for event family AD. *A*, Differential arrival times for 72 events in family AD indicate a very high degree of waveform similarity at stations AUP, AUH, AUW, and AUL. Differential times are calculated using the adjusted P-wave onset based on waveform crosscorrelation. The median value is noted. *B*, The residual time is calculated by removing the median for each station pair. The mean of the residuals for each station pair is 0.0 s, a strong indication that individual member events are collocated.

evidence for mixing between dacitic and more mafic source magma. Magma remained compositionally heterogeneous over the length of that eruption. They concluded that the 1986 eruption resulted from an injection of hot, mafic magma stored between 3 and 4 km b.m.s.l. This material mixed with more dacitic residual magma left in the edifice following the 1976 eruption. The source depth of 3 to 4 km is significantly deeper than the source constrained by cGPS modeling of the 2006 eruption, however. Both models suggest that magma storage and transport in the Augustine edifice takes place through a series of dikes, some of which are interconnected and some of which are not.

Volcano-tectonic (VT) seismicity caused by fluid and volatile transport is a commonly recorded feature of volcanoes before and during volcanic eruptions (for example, McNutt, 2005). Hill (1977) proposed that earthquake swarms result from the migration of fluids through a series of en echelon extension fractures linked to each other by small crack-tip shear fractures. Fracture mesh formation occurs within a constant stress field within a volume of rock, most favorably in materials with a high degree of heterogeneity and in the presence of low effective stress (Sibson, 1996), conditions likely to exist in a volcanic edifice. VT activity along the mesh

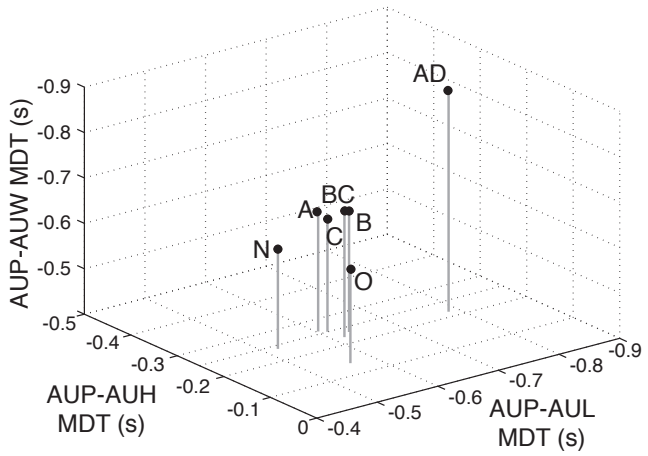

Figure 13. The median differential times (MDT) for a set of station-pairs for each family contain information on the relative location of event families in space. Here, the MDTs for station pairs AUP-AUH, AUP-AUL, and AUP-AUW are plotted for a number of well-recorded clusters occurring the 2006 eruption (see fig. 4*C* for family time ranges). On the basis of geometric arguments, family AD occurs higher in the edifice than the other families. Families C, BC, B, O, and N occur over the same period in early December but are not collocated on this diagram, indicating that multiple regions of the edifice can be simultaneously active.

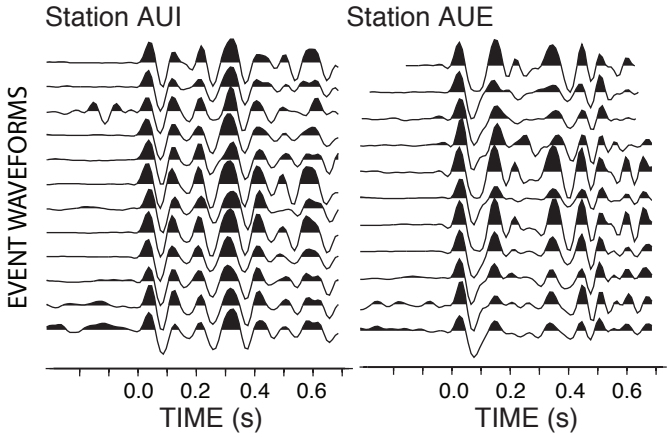

Figure 14. Waveforms for family AA, here shown at stations AUI and AUE, consist of deep earthquakes (~3 km b.m.s.l.) that occur from May through July 2006. All deep earthquakes in the AVO catalog occur in mid to late 2006. Only the flank stations recorded these earthquakes because of the timing.

of shear fractures could appear to be spatially and temporally variable (for example, Roman and Cashman, 2006), with small swarms of activity localizing on individual shears over shorter time scales. Magma transport through dike emplacement, as modeled for the 2006 Augustine eruption, can also generate VT swarms. Ukawa and Tsukahara (1996) suggested that VT swarm activity forms because of extension of wallrock ahead of a propagating dike tip. This model implies a spatial and temporal migration of seismicity in the direction of dike propagation. Roman (2005) showed that inflation of a dike would compress the surrounding wallrock and lead to generation of seismicity in a temporally and spatially random manner. Modeling suggests that seismicity caused by dike-tip propagation and by wallrock compression could be active at the same time (Roman and Cashman, 2006). Roman and Cashman (2006) compare seismicity and fault plane solutions at a number of volcanoes to each of the above models and conclude that at most compressive arc settings, the Roman (2005) and to a lesser extent the Hill (1977) model best explain recorded VT activity. Fracture mesh orientation would be controlled by the regional stress regime, while wallrock failure would reflect local perturbations to this regime. Well-constrained focal mechanism solutions can be used to distinguish between these two processes (Roman and Cashman, 2006).

Our observation that some waveforms repeat over multiple years suggests that in some regions of the edifice the VT source mechanism is nondestructive. Of the three models presented, this seems most consistent with the idea of shear failure along a fracture mesh. Volcanic edifices are fluid-rich and volatile-rich environments, and transport of materials within the edifice must constantly occur. Reported rates of fumoralic activity are fairly constant at Augustine. If transport does occur through a series of interconnected extension and shear fractures, periods of increased transport rate may lead to the periods of increased activity we identify as swarms making up individual event families. The mesh must evolve because of precipitation and mineralization within the fractures (Sibson, 1996). Seismicity not included in event families may be localized to shear fractures that form or reactivate variably in both space and time.

This interpretation does not preclude VT activity due to dike inflation or deflation within the edifice. If dikes are the primary magma transport and storage mechanism at Augustine, then wallrock adjustments due to volumetric changes in the existing dike complex may generate VT seismicity by locally perturbing the local stress field. Inflation may induce short-term compression in the surrounding wallrock and induce swarms of temporally and spatially related seismicity (Roman, 2005). Dike ascent during the precursory stage of the 2006 Augustine eruption is accompanied by increased seismicity rates (Cervelli and others, 2006; Mattia and others, 2008). If the ascending dike interacted with a preexisting dike network, as is posited for the 1986 Augustine eruption, then multiple dikes could have inflated or deflated over the course of the 2006 eruption. This may explain both the cloud-like pattern of dissimilar earthquakes that dominate the entire Augustine catalog and the swarms of highly similar waveforms generated during the 2006 eruption.

The largest identified swarms occurred as the ascending source dike reached near-surface elevations on December 9–11, 2005, and between explosive eruptions through January 2006 (fig. 4*C*). Locations of families identified during this period suggest that some seismicity generated over December 9–11, 2005, occurred ~700 to 800 m below the activity in January 2006 (this study; Sumiejski and others, 2009). We suggest that event families A, B, BC, and C are directly related to this ascending dike. All share similar waveform characteristics, such as frequency content and P onset sign (fig. 8), and the clusters are located very close to each other in space (fig. 13). However, we cannot distinguish if these swarms form because of failure along a propagating dike tip or within the surrounding wallrock during dike ascension. Cervelli and others (2006) and Mattia and others (2008) suggest that the ascending dike breaches the surface during the January 13, 2006, eruption. It is therefore likely that this dike causes the seismicity associated with the January 11 swarm (family AD). Seismicity occurring throughout the remainder of January is both related to summit activity (family AH) and to wallrock adjustments to changing pressures within the dike source at ~500 m a.m.s.l (family AC) (Sumiejski and others, 2009). Longer term magma storage may take place nearer ~300 m b.m.s.l. on the basis of modeling of cGPS data (for example, Mattia and others, 2008) recorded during the early precursory stage and the location of multiyear family LM (for example, Sumiejski and others, 2009).

Conclusions

Waveform similarity at Augustine volcano derived using waveform crosscorrelation techniques occurs over a number of time scales. Approximately 60 to 70 percent of volcano-tectonic events in the AVO catalog are not associated with event clusters containing more than 10 earthquakes. These events may be forming along shear fractures that form in conjunction with extension fractures and facilitate fluid movement within the volcanic edifice. Alternately, these events may reflect long-term wallrock failure caused by local stress perturbations associated with a series of interconnected storage dikes. Events forming families before the 2006 eruption exhibit a high degree of similarity over multiple years but generally consist of subsets of small temporally related swarms. These events would be consistent with either reactivation of shear fractures that form the fracture mesh systems or failure in wallrock near long-lived inflating or deflating dikes. Focal mechanisms would help distinguish between these two models.

Earthquakes recorded during the precursory phases of the 2006 eruption occur as swarms of similar earthquakes over periods of days or hours. The largest identified precursory swarms accompany reports of increased steaming and explosive eruptions at the summit, which are consistent with discrete dikes/sills opening to accommodate magma transport

to the surface. Some event families appear directly associated with an ascending dike through late November and December 2006, but we cannot say whether these events occur along a propagating dike tip or within the surrounding wallrock without focal-mechanism data. Other event families clearly occur at the same time as dike ascension but occur throughout the volcanic edifice, suggesting that local stress perturbations activate a network of fractures or preexisting dikes. Combined with the generally low degree of event similarity at Augustine, the seismic results agree well with the hypothesis that magma transport and storage during eruptions involves numerous dikes located throughout the edifice (Roman and Cashman, 2006; Cervelli and others, this volume; Larsen and others, this volume; Power and Lalla, this volume).

Seismicity rate and event similarity decrease rapidly over the course of the 2006 eruption. The only family identified during the late eruptive and effusive phases contains relatively deep earthquakes between 3 and 5 km b.m.s.l. If the source dike for the 2006 eruption ascends from 0 km b.m.s.l. or deeper, these events may reflect posteruptive magma transport at the base of the Augustine magmatic system.

Acknowledgments

We thank James Dixon and the Alaska Volcano Observatory for access to waveform and pick data. Waveforms, shot locations and times, and parametric data from the active source experiment were obtained from the IRIS DMC. Stephanie Prejean provided helpful discussions. We thank Jeffery Freymueller, Charlotte Rowe, and Maurizio Battaglia for insightful reviews. Waveforms, picks, and crosscorrelation data reported in this study may be obtained by request through Heather DeShon. The material is based on research supported by NSF grant EAR-0409291 to Clifford Thurber.

References Cited

Aster, R.C., and Rowe, C.A., 2000, Automatic phase pick refinement and similar event association in large seismic datasets, *in* Thurber, C.H., and Rabinowitz, N., eds, Advances in seismic event location: Kluwer, Amsterdam, p. 231–263.

Battaglia, J., Thurber, C.H., Got, J.L., Rowe, C.H., and White, R.A, 2004, Precise relocation of earthquakes following the 15 June 1991 eruption of Mount Pinatubo, Philippines: Journal of Geophysical Research, v. 109, B07302, doi:10.1029/2003JB002959.

Buurman, H., and West, M.E., 2010, Seismic precursors to volcanic explosions during the 2006 eruption of Augustine Volcano, *in* Power, J.A., Coombs, M.L., and Freymueller, J.T., eds., The 2006 eruption of Augustine Volcano, Alaska: U.S. Geological Survey Professional Paper 1769 (this volume).

Cervelli, P.F., Fournier, T., Freymueller, J., and Power, J.A., 2006, Ground deformation associated with the precursory unrest and early phases of the January 2006 eruption of Augustine Volcano, Alaska: Geophysical Research Letters, v. 33, L18304, 10.1029/2006GL027219.

Cervelli, P.F., Fournier, T.J., Freymueller, J.T., Power, J.A., Lisowski, M., and Pauk, B.A., 2010, Geodetic constraints on magma movement and withdrawal during the 2006 eruption of Augustine Volcano, *in* Power, J.A., Coombs, M.L., and Freymueller, J.T., eds., The 2006 eruption of Augustine Volcano, Alaska: U.S. Geological Survey Professional Paper 1769 (this volume).

DeShon, H.R., Thurber, C.H., and Rowe, C., 2007, High-precision earthquake location and three-dimensional P wave velocity determination at Redoubt Volcano, Alaska: Journal of Geophysical Research, v. 112, B07312, doi:10.1029/2006JB004751.

Dixon, J.P., Stihler, S.D., Power, J.A., and Searcy, C., 2008, Catalog of earthquake hypocenters at Alaskan volcanoes; January 1 through December 31, 2006: U.S. Geological Survey Data Series 326, 78 p.

Dodge, D.A., 1996, Xadjust; a Matlab-based cross correlation analysis package: Seismological Research Letters, v. 67, p. 36.

Dodge, D.A., Beroza, G.C., and Ellsworth, W.L., 1995, Foreshock sequence of the 1992 Landers, California, earthquake and its implications for earthquake nucleation: Journal of Geophysical Research, v. 100, p. 9865–9880.

Du, W., Thurber, C.H., and Eberhart-Phillips, D., 2004, Earthquake relocation using cross correlation time delay estimates verified with the bispectrum method: Bulletin of the Seismological Society of America, v. 94, p. 856–866.

Got, J.L, Frechet, J., and Klein, F.W., 1994, Deep fault plane geometry inferred from multiplet relative relocation beneath the south flank of Kilauea: Journal of Geophysical Research, v. 99, p. 15375–15386.

Hill, D.P., 1977, A model for earthquake swarms: Journal of Geophysical Research, v. 82, p. 1347–1352.

Kienle, J., 1987, Mt. St. Augustine works, but how? [abs.]: Hawaii Symposium on How Volcanoes Work, Abstract Volume, p. 139.

Lalla, D.J., and Kienle, J., 1980, Problems in volcanic seismology on Augustine Volcano, Alaska [abs.]: Eos (Transactions American Geophysical Union), v. 61, p. 68.

Larsen, J.F., Nye, C.J., Coombs, M.L., Tilman, M., Izbekov, P., and Cameron, C., 2010, Petrology and geochemistry of the 2006 eruption of Augustine Volcano, *in* Power, J.A.,

Coombs, M.L., and Freymueller, J.T., eds., The 2006 eruption of Augustine Volcano, Alaska: U.S. Geological Survey Professional Paper 1769 (this volume).

Mattia, M., Palano, M., Aloisi, M., Bruno, V., and Bock, Y., 2008, High rate GPS data on active volcanoes; an application to the 2005-2006 Mt. Augustine (Alaska, USA) eruption: Terra Nova, v. 20, no. 2, p. 134–140.

McNutt, S.R., 2005, Volcanic seismology: Annual Reviews of Earth and Planetary Science, v. 33, p. 461–491.

Milne, J., 1886, Earthquakes and other earth movements: New York, D. Appleton and Company, 363 p.

Nikias, C.L., and Pan, R., 1988, Modeling of the 4th-order cumulants and phase estimation: Circuits Systems Signal Processing, v. 7, p. 291–325.

Nikias, C.L., and Raghuveer, M.R., 1987, Bispectrum estimation—a digital signal-processing framework: Proceedings of the IEEE, v. 75, p. 869–891.

Power, J.A., 1988, Seismicity associated with the 1986 eruption of Augustine Volcano, Alaska: Fairbanks, University of Alaska, M.S. thesis, 142 p.

Power, J.A., and Lalla, D.J., 2010, Seismic observations of Augustine Volcano, 1970–2007, *in* Power, J.A., Coombs, M.L., and Freymueller, J.T., eds., The 2006 eruption of Augustine Volcano, Alaska: U.S. Geological Survey Professional Paper 1769 (this volume).

Roman, D.C., 2005, Numerical models of volcanotectonic earthquake triggering on non-ideally oriented faults: Geophysical Research Letters, v. 32, L02304, doi:10.1029/2004GL021549.

Roman, D.C., and Cashman, K.V., 2006, The origin of volcano-tectonic earthquake swarms: Geology, v. 34, p. 457–460.

Roman, D.C., Cashman, K.V., Gardner, C.A., Wallace, P.J., and Donovan, J.J., 2006, Storage and interaction of compositionally heterogeneous magmas from the 1986 eruption of Augustine Volcano, Alaska: Bulletin of Volcanology, v. 68, p. 240–254, doi:10.1007/s00445-005-003-z.

Rowe, C.A., 2000, Correlation-based phase pick corrections and similar earthquake family identification in large seismic waveform catalogs: Socorro, New Mexico Institution of Mining & Technology, Ph.D. Thesis, 187 p.

Rowe, C.A., Aster, R.C., Borchers, B., and Young, C.J., 2002a, An automatic, adaptive algorithm for refining phase picks in large seismic datasets: Bulletin of the Seismological Society of America, v. 92, p. 1660–1674.

Rowe, C.A., Aster, R.C., Phillips, W.S., Borchers, B., Jones, R.H., and Fehler, M.C., 2002b, Using automated, high-precision repicking to improve delineation of microseismic structures at the Soultz geothermal reservoir: Pure and Applied Geophysics, v. 159, p. 563–596.

Rowe, C.A., Thurber, C.H., and White, R.A., 2004, Dome growth behavior at Soufriere Hills Volcano, Montserrat, revealed by relocation of volcanic event swarms, 1995-1996: Journal of Volcanology and Geothermal Research, v. 134, p. 199–221.

Rubin, A.M., Gillard, D., and Got, J.L., 1998, A reinterpretation of seismicity associated with the January 1983 dike intrusion at Kilauea Volcano, Hawaii: Journal of Geophysical Research, v. 103, p. 10003–10015.

Schaff, D.P., Bokelmann, G.H.R., Beroza, G.C., Waldhauser, F., and Ellsworth, W.L., 2002, High-resolution image of Calaveras Fault seismicity: Journal of Geophysical Research, v. 107, p. 2186, doi:10.1029/2001JB000633.

Shearer, P.M., 1998, Evidence from a cluster of small earthquakes for a fault at 18 km depth beneath Oak Ridge, southern California: Bulletin of the Seismological Society of America, v. 88, p. 1327–1336.

Sibson, R.H., 1996, Structural permeability of fluid-driven fault-fracture meshes: Journal of Structural Geology, v. 18, p. 1031–1042.

Sumiejski, L., Thurber, C., and DeShon, H.R., 2009, Relocation of eruption-related earthquake clusters at Augustine Volcano, Alaska, using station-pair differential times: Geophysical Journal International, v. 176, p. 1017–1022.

Ukawa, M., and Tsukahara, H., 1996, Earthquake swarms and dike intrusions off the east coast of Izu Peninsula, central Japan: Tectonophysics, v. 253, p. 285–303, doi:10.1016/0040-1951(95)00077-1.

Wallace, K.L., Neal, C.A., and McGimsey, R.G., 2010, Timing, distribution, and character of tephra fall from the 2005–2006 eruption of Augustine Volcano, *in* Power, J.A., Coombs, M.L., and Freymueller, J.T., eds., The 2006 eruption of Augustine Volcano, Alaska: U.S. Geological Survey Professional Paper 1769 (this volume).

Yung, S.K., and Ikelle, L.T., 1997, An example of seismic time picking by third-order bicoherence: Geophysics, v. 62, p. 1947–1952.

Zhou, H., 1994, Rapid three-dimensional hypocentral determination using a master station method, Journal of Geophysical Research: v. 99, p. 15439–15455.